

Self-Assembly of Gold Nanoparticles Utilizing a Charge-Transfer Interaction between Carbazolyl and Dinitrophenyl Units

Kensuke Naka,* Hideaki Itoh, and Yoshiki Chujo*

Department of Polymer Chemistry, Graduate School of Engineering, Kyoto University, Katsura, Nishikyo-ku, Kyoto 615-8510

Received March 17, 2004; E-mail: ken@chujo.synchem.kyoto-u.ac.jp

Colloidal gold nanoparticles self-assembled into macroscopic aggregates by a charge-transfer interaction between a 9-carbazolyl unit as an electron-donor immobilized on the surface of the gold nanoparticles and a bivalent linker containing two dinitrophenyl units as electron-acceptors. Transmission electron microscopy and scanning electron microscopy images showed spherical aggregates consisting of the gold nanoparticles.

Metal nanoparticles have been extensively studied for decades. They have a wide functional diversity very different from bulk materials, with much of their electronic,[1] optical,[2] and catalytic[3] properties originating from their quantum-scale dimensions. Their unique properties are of potential utility in chemical sensing, linear and nonlinear optics, and in a variety of nanoscale electronic devices. That is, metal nanoparticles should become essential building blocks for advanced devices. In order to progress toward these applications, ways to organize the nanoparticles into controlled architectures, such as one-, two-, and three-dimensional arrangements, must be found. One of the more efficient methodologies for organizing metal nanoparticles involves self-assembly based on selective control of non-covalent interactions. Several approaches (hydrogen-bonding interaction,[4] π–π interaction,[5] host–guest interaction,[6] van der Waals forces,[7] electrostatic forces,[8] antibody–antigen recognition[9]) have been described concerning the formation of arrays of metal nanoparticles. These results have provided a powerful method for employing pre-programmed materials with the potential for multi-dimensional ordering for the creation of well-defined structures at the molecular level. The organization of metal nanoparticles in superstructures of desired shape and morphology is a challenging research area.

Recently, we have reported on the self-assembly of colloidal gold nanoparticles into macroscopic aggregates by a charge-transfer interaction (CT interaction) between a pyrenyl unit as an electron-donor immobilized on the surface of gold nanoparticles and a bivalent linker containing two dinitrophenyl units as electron-acceptors.[10] This methodology allows the gold nanoparticles to self-assemble reversibly into aggregates by controlling the temperature. One of the advantages of this system is that the binding strength can be easily tailored by modifying the structure of the electron-donor and electron-acceptor moieties, since the stability of CT complexes also depend on the structure of the components of the CT complexes. We expected that the size and shape of a nanoparticle assembly would be controlled through turning the structure of the components of the CT complexes.

In order to obtain detailed knowledge about the effect of a CT complex for a self-assembly process, here, we utilized different combinations of CT complexes between a 9-carbazolyl unit as an electron-donor and dinitrophenyl units as electron-acceptors in this system (Fig. 1). The addition of a bivalent linker to a solution of individual gold nanoparticles resulted in the formation of macroscopic aggregates comprising noncovalently linked gold nanoparticles through the CT interaction.

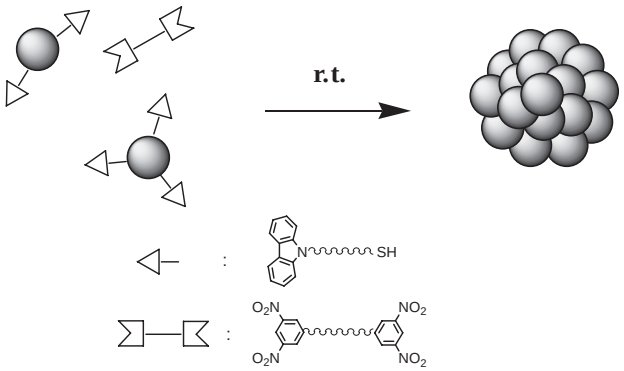

Fig. 1. Schematic illustration for thermally reversible self-assembly of metal nanoparticles by charge-transfer interaction.

Results and Discussion

Synthesis of Gold Nanoparticles. Gold nanoparticles were prepared by the reduction of $HAuCl_4$ (20.0 mg, 0.048 mmol) with $NaBH_4$ in the presence of 11,11′-dithiobis(undecanoic acid 2-(9-carbazolyl)ethyl ester) (**1**) (10 mg, 1.2×10^{-2} mmol). The UV–vis absorption spectrum of a red solution after chemical reduction with $NaBH_4$ indicated the formation of gold nanoparticles with a surface plasmon absorption band at 500 nm.

The average diameter of the **1**-modified gold nanoparticles was 2.12 ± 1.1 nm, as measured by transmission electron microscopy (TEM) (Fig. 2).

Figure 3 shows the ^{1}H NMR spectra of **1** and the **1**-modified gold nanoparticles in $CDCl_3$. In the ^{1}H NMR of the **1**-modified

Published on the web March 11, 2005; DOI 10.1246/bcsj.78.501

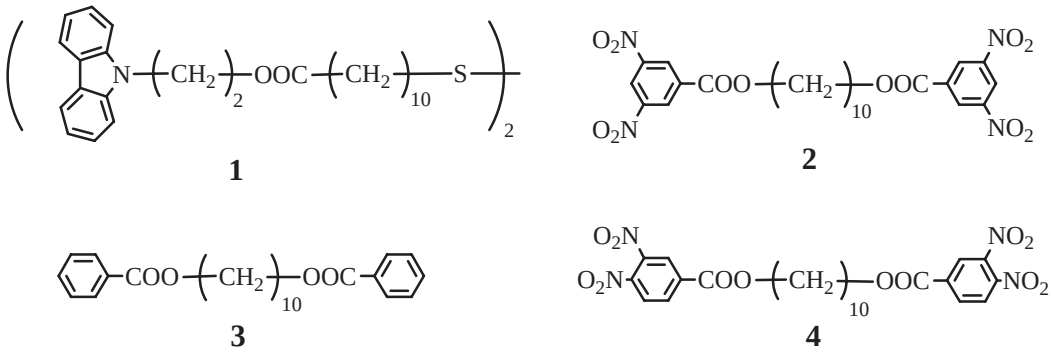

Chart 1.

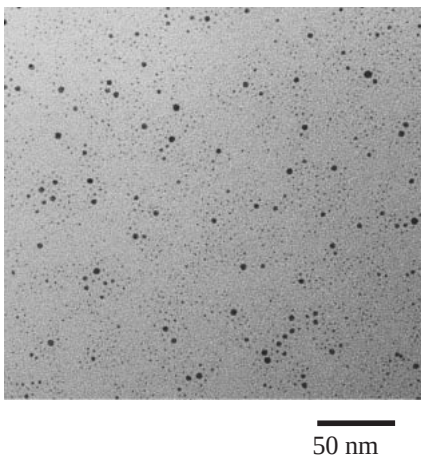

Fig. 2. TEM image of the **1**-modifed gold nanoparticles.

gold nanoparticles signals appeared corresponding to those of the proton signals of the parent **1** (Fig. 3b). The signals of the methylene protons in the **1**-modified gold nanoparticles are broadened and shifted compared to those of **1**. The signals of methylene protons closest to the thiolate/Au interface can be hardly recognized, since the motion of the methylene groups close to the surface of the gold nanoparticles was constrained. This type of signal broadening was observed in bipyridyl or alkanethiolate-modified metal nanoparticles.[11] These results indicate clear evidence for the attachment of thiolated carbazole to the surface of the gold nanoparticles.

Assembly of Nanoparticles in the Presence of Linkers. A bivalent 3,5-dinitrophenyl linker (**2**) was added to a benzene solution of **1**-modified gold nanoparticles at room temperature. The solution color gradually faded with increasing the incubation time. The reaction of the **1**-modified gold nanoparticles with **2** was followed as a function of time through optical changes in the surface plasmon band in the UV–vis absorption spectrum. After the addition of **2**, a broadening in the surface plasmon resonance was observed. The absorption of the surface plasmon band was almost saturated at 24 h after the addition of **2**. Figure 4 shows the UV–vis absorption spectrum recorded at 24 h after the addition of **2** with varying concentrations to colloidal solutions of the **1**-modified gold nanoparticles. Decreasing in the surface plasmon band became more significant with increasing the concentrations of **2**, indicating the formation of particle aggregates.[6] The UV–vis absorption

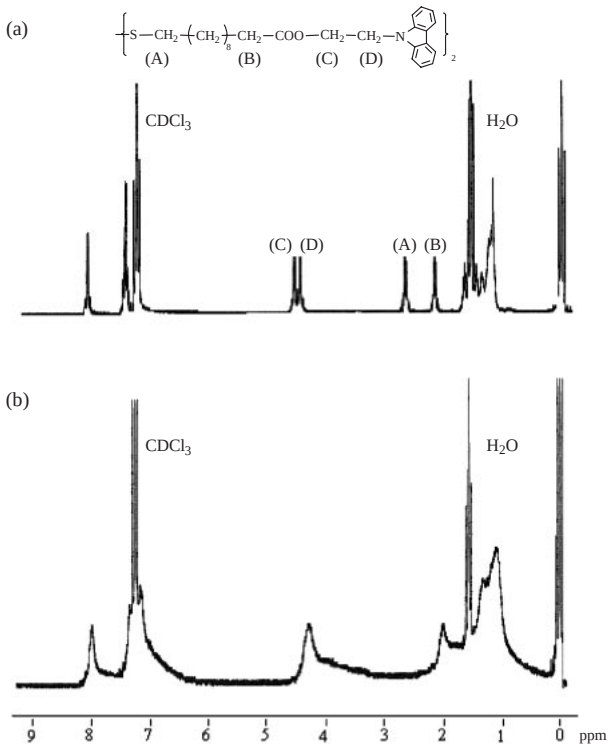

Fig. 3. ^{1}H NMR spectra of (a) **1** and (b) the **1**-modified gold nanoparticles.

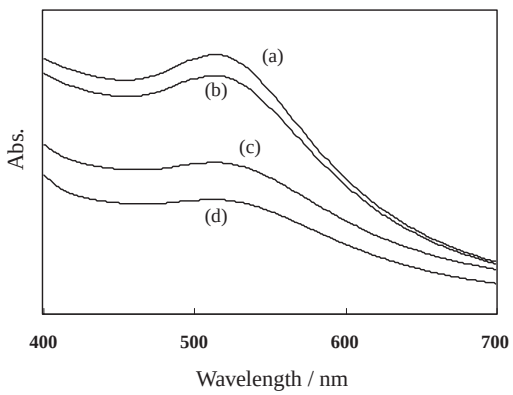

Fig. 4. UV–vis absorption spectra by changing the weight ratio of **2** against the **1**-modified gold nanoparticles. **2**/**1**-modified gold nanoparticles = (a) 0, (b) 1, (c) 5, (d) 10.

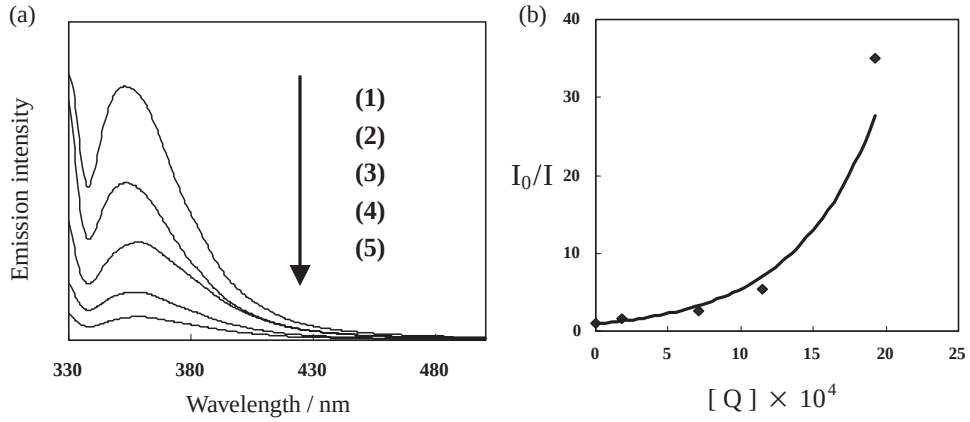

Fig. 5. (a) Fluorescence quenching of carbazolyl units on the surface of the gold nanoparticles by **5** in toluene ($\lambda_{ex} = 330$ nm). The concentration of **5** at decreasing emission intensities are (1) 0.0 M, (2) 1.76×10^{-4} M, (3) 7.08×10^{-4} M, (4) 1.15×10^{-3} M, (5) 1.93×10^{-3} M. (b) Stern–Volmer plots of the fluorescence quenching by **5** in toluene in the presence of the **1**-modified gold nanoparticles. I_0 and I represent the emission intensities in the absence and presence of **5**, respectively.

spectrum showed no change for several days. This indicates that the obtained aggregates maintained their size at room temperature.

Two control experiments provided additional insights into the correlation of the spectral evolution. First, to confirm the recognition property between the carbazolyl units and the dinitrophenyl units, we used 1,10-decanediyl dibenzoate (**3**) with two benzoate groups, which showed no interaction with the dinitrophenyl units. In contrast to the results obtained with **2**, the addition of **3** to a solution of the **1**-modified gold nanoparticles caused no color change and no change in the UV–vis absorption spectrum. This result indicates that the self-assembly of the **1**-modified gold nanoparticles proceeded through a specific CT interaction. Second, a colorimetric change was not detectable using 1,3-dinitrobenzene instead of **2** for the solution of the **1**-modified gold nanoparticles, which showed a requirement of the bivalent linker for aggregation. These results clearly indicate that the **1**-modified gold nanoparticles aggregated through cross-linking by **2**, which recognized carbazolyl residues on the surface of the gold nanoparticles.

Fluorescence Quenching. According to literature,[12] the CT band between carbazole and dinitrobenzene is observed around 450 nm, which shows a complete overlap with the spectra of the surface plasmon band of the gold nanoparticles. Thus, the UV–vis absorption spectrum gave no clear proof of the presence of the CT complex. To confirm the presence of the CT interaction in the present system, a fluorescence measurement was carried out. Figure 5a shows the quenching of the carbazolyl units on the gold nanoparticles by **5** as a model compound of **2** in toluene at 25 °C to eliminate the effect of the particle aggregates. As the concentration of **5** increased, the emission intensity decreased without any change in the spectral pattern. This indicates that the quenching process occurred via charge transfer from the carbazolyl units to the dinitrophenyl units. No exciplex emission was detectable in the spectral region under these experimental conditions. Stern–Volmer plots of the carbazolyl units of the fluorescence quenching using **5** are shown in Fig. 5b. The plots are not linear, indicating a static-type quenching mechanism via a ground-state complex formation. The static quenching mechanism was substantiated by studying the temperature effect on the fluorescence quenching efficiency.

TEM Image of the Assembly of Gold Nanoparticles. TEM was used to characterize the aggregates. One drop of a solution containing the obtained product was placed on a copper grid and allowed to evaporate the solvent under atmospheric pressure at room temperature. Although the TEM image before the addition of **2** showed well-separated gold nanoparticles with an uniform size distribution (Fig. 2), the TEM image measured at 24 h after the addition of **2** (5 mg) to a toluene solution containing the **1**-modified gold nanoparticles (1 mg) showed the formation of large, spherical aggregates with a diameter of 1.5 ± 0.7 μm (Fig. 6a). The microscopic aggregates consisted of individual gold nanoparticles. When a TEM image was measured at 6 h after the addition of **2** (5 mg), a spherical aggregate with an average diameter of 200 nm, in addition to smaller aggregates, was observed. The addition of 1 mg and 10 mg of **2** resulted in the formation of spherical aggregates with diameters of 34 nm and 3.5 ± 1.2 μm, respectively. Thus, the degree of colloidal association would be controlled by adjusting the concentration of **2** in the medium.

Equilibrium Constants. The stability of the CT complexes depends on the structure of the dinitrophenyl unit. To confirm the effect of the acceptor strength, 1,10-decanediyl bis(3,4-dinitrobenzoate) (**4**) with *o*-dinitrophenyl units at each end was used. In contrast to the results obtained with **2**, the addition of **4** to the solution of the **1**-modified gold nanoparticles showed no change in the UV–vis absorption spectrum, indicating no aggregate formation of the gold nanoparticles by **4**. The absorption of the CT complexes was neglected compared with that of the gold nanoparticles in a UV–vis absorption measurement. To determine the equilibrium constants (K_c) of the CT complex, **5**, **6**, and **7** were, thus, employed as model compounds for **2**, **4**, and **1**, respectively. The absorption spectra of mixed solutions with a fixed concentration of **7** and varying concentrations of **5** and **6** in toluene at room temperature are shown in Fig. 7. The absorbance of the broad absorption band, which can be seen up to 500 nm in Fig. 7, increased with an increase in the concentration of **7** as the donor compound. This band is ascribed to the CT complex of **5** or **6** with **7**. A com-

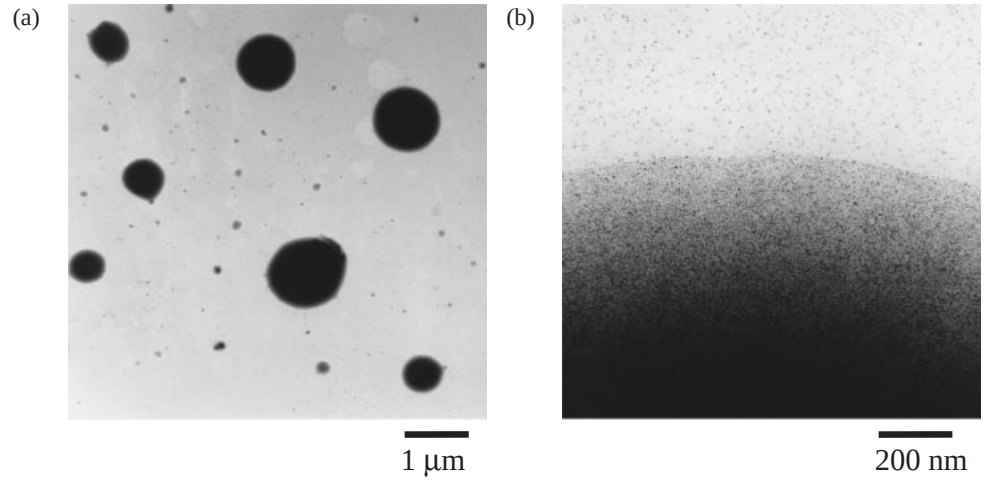

Fig. 6. (a) TEM image and (b) magnified TEM image of the spherical aggregates of the **1**-modified gold nanoparticles.

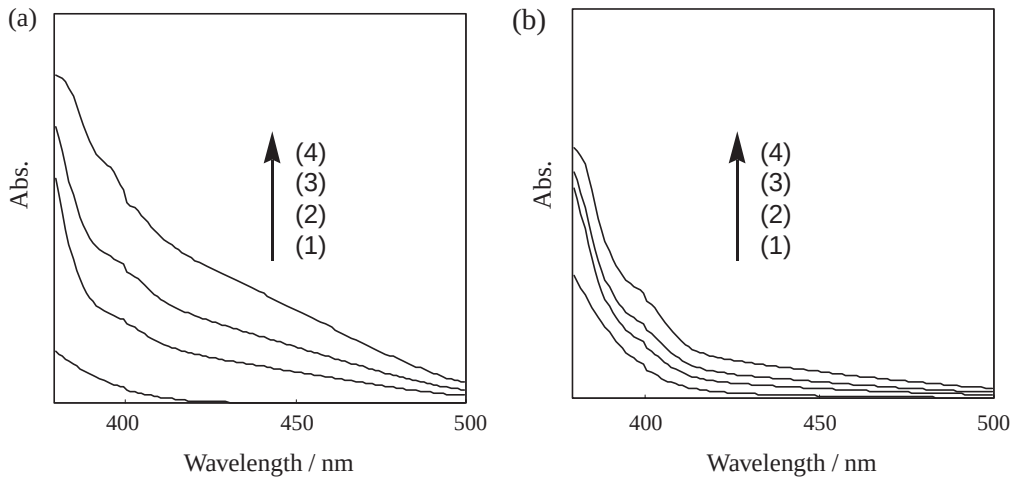

Fig. 7. (a) UV–vis absorption spectra of the CT complexes between **5** and **7**. The concentrations of **7** (solid line) are (1) 0 M, (2) 3.42×10^{-2} M, (3) 6.92×10^{-2} M, (4) 12.6×10^{-2} M. The concentration of **5** is 8.85×10^{-3} M. (b) UV–vis absorption spectra of the CT complexes between **6** and **7**. The concentrations of **7** (solid line) are: (1) 0 M, (2) 3.51×10^{-2} M, (3) 7.12×10^{-2} M, (4) 12.4×10^{-2} M. The concentration of **6** is 8.85×10^{-3} M.

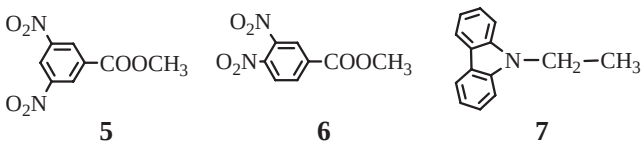

Chart 2.

parison of Figs. 7a and 7b revealed that the increase of the absorption band in Fig. 7a was larger than that in Fig. 7b. These results suggest that the K_c values of the CT complexes with a carbazolyl group decreased in the order of 3,5-dinitrophenyl group > 3,4-dinitrophenyl group. The Rose and Drago equation[13] was used to calculate the K_c value of the CT complex from the spectrophotometric data. The order of the K_c values of the CT complexes of different acceptors with **7** appeared to be **5** ($K_c = 2.2$) > **6** ($K_c = 1.1$). This difference in the equilibrium constants of the CT complex reflects the assembly process. These results clearly show control of the self-assembly process by turning the structure of the acceptor compounds. Based on the K_c value of the CT complex of **5** and **7**, we presume that 4% and 1% of the carbazolyl units on the gold nanoparticles formed the CT complex with **2** after the addition of 5 mg and 1 mg of **2**, respectively.

Effect of the CT Complex for Self-Assembly Process. The present result was compared with a previous result using the CT complex between the pyrenyl unit and the dinitrophenyl unit. The equilibrium constant (K_s) of the CT complex between the carbazolyl unit and the dinitrophenyl unit is 2.2. This value is smaller than that of the CT complex between the pyrenyl unit and the dinitrophenyl unit ($K_s = 11.2$) in the previous result.[10] Based on the comparison of these equilibrium constants, we expect that the aggregation of the **1**-modified gold nanoparticles via the CT complex between the pyrenyl unit and the dinitrophenyl unit is efficient compared with the CT complex between the carbazolyl unit and the dinitrophenyl unit. A TEM investigation using the CT complex between the pyrenyl unit and the dinitrophenyl unit demonstrated that

spherical aggregates with a diameter of 1 ± 0.7 μm were observed at a feed weight ratio of the **2**/**1**-modifed gold nanoparticles = 1. Compared with the previous result, the size of spherical aggregates (34 nm) at the same feed weight ratio is small. That is, the stronger CT interaction results in the formation of larger spherical aggregates. The described experimental results were in accordance with the expectation based on the equilibrium constants of the CT complex, demonstrating control of the aggregate process by turning the CT complex.

Conclusion

In conclusion, we have demonstrated the self-assembly of nanoparticles into macroscopic aggregates by the CT interaction. The shape of the macroscopic aggregates formed using this strategy is regular and spherical. The ability to tailor the binding strength by this methodology would be highly desirable in many applications. The present results suggest that the self-assembly process of gold nanoparticles is controlled through turning the structure of the acceptor compounds. We expect that this concept represents a powerful and general strategy for the creation of highly structured multifunctional materials.

Experimental

Materials. All solvents and reagents were obtained from commercial sources and used as supplied except for the following. Tetrahydrofuran (THF) was distilled under nitrogen.

Measurement. ^{1}H NMR spectra were obtained with a JOEL JNM-EX270 spectrometer (270 MHz for ^{1}H NMR) in chloroform-*d*. UV–visible spectra were measured on a Jasco V-530 spectrometer. Transmission electron microscopy was performed using a JOEL JEM-100SX operated at 100 kV. Scanning electron microscopy was performed using a JOEL JNM-5310/LV system. Fluorescence emission spectra were recorded on a Perkin-Elmer LS 50B luminescence spectrometer.

11,11′-Dithiobis(undecanoic Acid). To a solution of 11-mercaptoundecanoic acid (200 mg, 0.92 mmol) in H_2O (100 mL) was added sodium hydroxide (500 mg, 12.5 mmol). A hydrogen peroxide solution (2 mL) was added to a well-stirred resulting mixture. After being stirred for 30 min, concentrated HCl (2 mL) was added and the mixture was extracted with ethyl acetate several times. The organic portion was washed with saturated aqueous NaCl and dried over $MgSO_4$. After removing the solution, disulfide was obtained as a colorless solid (110 mg, 55% yield). ^{1}H NMR (DMSO): δ 1.23–1.35 (12H, m), 1.46 (2H, t), 1.57 (2H, t), 2.26 (2H, t), 2.69 (2H, t).

11,11′-Dithiobis(undecanoic Acid 2-(9-Carbazolyl)ethyl Ester) (1). To a solution of 1-pyrenebutanol (1.0 g, 3.64 mmol) in $CHCl_3$ was added 11,11′-dithiobis(undecanoic acid) (0.7 g, 1.61 mmol), dicyclohexylcarbodiimide (1.0 g, 4.85 mmol), and 4-dimethylaminopyridine (0.06 g, 0.49 mmol). The mixture was stirred at room temperature for 24 h. After removing the precipitate by filtration, the solution was evaporated under reduced pressure. The remaining white solid was subjected to column chromatography. The first fraction containing the product was concentrated by evaporation and dried under reduced pressure; **1** was obtained (20%). ^{1}H NMR ($CDCl_3$) δ 1.12–1.41 (12H, m), 1.65 (4H, m), 1.80 (2H, t), 1.94 (2H, t), 2.27 (2H, t), 2.64 (2H, t), 3.38 (2H, t), 4.14 (2H, t), 7.84–8.26(9H, m). Anal. Calcd for $C_{50}H_{64}N_2O_4S_2$ (821.17): C, 73.13; H, 7.86; O, 7.79; S, 7.81; N, 3.41%. Found: C, 73.08; H, 7.88; O, 7.74; S, 7.88; N, 3.42%.

1,10-Decanediyl Bis(3,5-dinitrobenzoate) (2), 1,10-Decanediyl Dibenzoate (3), 1,10-Decanediyl Bis(3,4-dinitrobenzoate) (4), Methyl 3,5-Dinitrobenzoate (5), and Methyl 3,4-Dinitrobenzoate (6). These compounds were synthesized according to a previous paper.[10]

Colloid Synthesis. Gold nanoparticles were prepared according to a procedure described by Brust.[14] $HAuCl_4$ (20.0 mg, 0.048 mmol) was dissolved in 30 mL of H_2O. Tetraoctylammonium bromide (26.5 mg, 0.048 mmol) was then added as a solution in 30 mL of toluene, and the reaction mixture was stirred until the yellow aqueous layer was clear and the organic layer was red. **1** (10 mg, 1.2×10^{-2} mmol) was then added, followed by the dropwise addition of $NaBH_4$ (5.23 mg, 0.14 mmol) as a solution in 5 mL of H_2O. This caused an immediate color change to dark black. The reaction mixture was stirred for 10 min, and the organic phase was collected and added to MeOH (100 mL). The precipitates were isolated by centrifugation. Gold nanoparticles stabilized by **1** were obtained as a black powder.

References

1 R. F. Khairutdinov, *Collloid J.*, **59**, 535 (1997).

2 a) P. Mulvaney, *Langmuir*, **12**, 788 (1996). b) A. P. Alivisatos, *J. Phys. Chem.*, **100**, 13226 (1996). c) K. G. Thomas, B. I. Ipe, and P. K. Sudeep, *Pure Appl. Chem.*, **74**, 1731 (2002).

3 A. Roucoux, J. Schulz, and H. Patin, *Chem. Rev.*, **102**, 3757 (2002).

4 a) A. K. Boal, F. Llhan, J. E. Derouchey, T. Thurn-Albrecht, T. P. Russell, and V. M. Rotello, *Nature*, **404**, 746 (2000). b) A. K. Boal and V. M. Rotello, *J. Am. Chem. Soc.*, **122**, 734 (2000). c) J. J. Storhoff, A. A. Lazarides, R. C. Mucic, C. A. Mirkin, R. L. Letsinger, and G. C. Schatz, *J. Am. Chem. Soc.*, **122**, 4640 (2000).

5 J. Jin. T. Iyoda, C. Cao, Y. Song, L. Jiang, T. J. Li, and D. B. Zhu, *Angew. Chem., Int. Ed.*, **40**, 2135 (2001).

6 a) J. Liu, S. Mendoza, E. Roman, M. J. Lynn, R. Xu, and A. E. Kaifer, *J. Am. Chem. Soc.*, **121**, 4304 (1999). b) S. Y. Lin, S. W. Liu, C. M. Lin, and C. H. Chen, *Anal. Chem.*, **74**, 330 (2002).

7 V. Patil, K. S. Mayya, S. D. Pradhan, and M. Sastry, *J. Am. Chem. Soc.*, **119**, 9281 (1997).

8 F. Caruso, R. A. Caruso, and H. Mohwald, *Science*, **282**, 1111 (1998).

9 W. Shenton, W. A. Davis, and S. Mann, *Adv. Mater.*, **11**, 449 (1999).

10 K. Naka, H. Itoh, and Y. Chujo, *Langmuir*, **19**, 5496 (2003).

11 a) M. J. Hostetler, J. E. Wingate, J. E. Harris, R. W. Vachet, M. R. Clark, J. D. Londono, S. J. Green, J. J. Stokes, G. D. Wignall, G. L. Glish, M. D. Porter, N. D. Evans, and R. W. Murray, *Langmuir*, **14**, 17 (1998). b) K. Naka, M. Yaguchi, and Y. Chujo, *Chem. Mater.*, **11**, 849 (1999).

12 Y. Shimazaki, M. Mitsuishi, S. Ito, and M. Yamamoto, *Langmuir*, **14**, 2768 (1998).

13 N. J. Rose and R. S. Drago, *J. Am. Chem. Soc.*, **81**, 6138 (1959).

14 M. Brust, M. Walker, D. Bethel, D. J. Schiffrin, and R. Whyman, *J. Chem. Soc., Chem. Commun.*, **1994**, 801.